ARMA 12-589

Time-lapse Passive Seismic Velocity Tomography of Longwall Coal Mines: A Comparison of Methods

Westman, E. C., Luxbacher, K. D., and Schafrik S. J.
Mining and Mineral Engineering Department, Virginia Tech, Blacksburg, VA, USA
Swanson, P. I.
Spokane Research Laboratory, NIOSH, Spokane, WA, USA
Zhang, H.
University of Science and Technology of China, Hefei, Anhui, P.R. China

Copyright 2012 ARMA, American Rock Mechanics Association

This paper was prepared for presentation at the 46th US Rock Mechanics / Geomechanics Symposium held in Chicago, IL, USA, 24-27 June 2012.

This paper was selected for presentation at the symposium by an ARMA Technical Program Committee based on a technical and critical review of the paper by a minimum of two technical reviewers. The material, as presented, does not necessarily reflect any position of ARMA, its officers, or members. Electronic reproduction, distribution, or storage of any part of this paper for commercial purposes without the written consent of ARMA is prohibited. Permission to reproduce in print is restricted to an abstract of not more than 300 words; illustrations may not be copied. The abstract must contain conspicuous acknowledgement of where and by whom the paper was presented.

ABSTRACT: Bumps in underground coal mines are violent events that result from a buildup of stress, usually in mines underlain and overlain by massive strata. Seismic velocity tomography can be implemented to infer stress distribution at mines and determine when a dangerous situation is developing. Three different methods were employed to compare time-lapse passive seismic tomograms at a longwall coal mine. The dataset is well sampled with a dense receiver array. Parameterization and results were compared using GeoTom, TomoDD, and SIMULPS. TomoDD and SIMULPS both allow for variable gridding and relocation of microseismic events while GeoTOM does not. All three methods produced consistent results for the data set showing clear high velocity zones in areas where abutment stress is expected and low velocity zones corresponding with gob. TomoDD proved to be the most suitable method for generating tomograms from mining-induced microseismic events because it resulted in the most consistent images and the calculated velocity distribution matched prior stress distribution measurements at the site.

1. INTRODUCTION

Seismic velocity tomography has been utilized previously in underground mines to produce velocity images that are used to infer stress redistribution. However, long-term passive seismic tomography is still a relatively immature, though promising, technology for the remote and continuous monitoring of a mine on a global scale using mining-induced microseismic events as sources. A high ratio of fatalities occurring in coal mines are the result of fall of roof, rib, or highwall. The tragic accident at Crandall Canyon increased awareness of the need for improved stress monitoring. The ultimate goal of this research effort is to do all that is possible to ensure the safety of the underground miner. The use of passive seismic tomography may be able to detect areas of relatively high stress in a mine so that precautionary measures can be taken, improving safety for miners working underground and positively impacting productivity. In order to implement passive seismic velocity tomography three methods of tomographic inversion are explored to determine which method provides the most consistent and meaningful results.

2. BACKGROUND

2.1. Tomography

Tomography gained recognition as a medical diagnostic tool [1] but also has many other applications. A tomogram is produced by propagating energy through some mass - a human body, a metal structure, or a rock mass, for example, and then measuring some response of the energy through the mass. These measurements can then be used to produce an image of the interior of the body. Passive seismic velocity tomography utilizes mining induced microseismic events as the energy sources and measures the p-wave arrival time of the seismic wave after it passes through the rock mass. The p-wave is the first part of the seismic wave to arrive and generally the easiest to measure. Next, the rock mass is discretized into three-dimensional cubes, or voxels, and a velocity is assigned to each voxel based on the time a segment of the seismic ray took to pass through the voxel, producing a three-dimensional model that can be sliced in areas of interest.

The premise of velocity tomography is that the seismic wave velocity through the rock mass is closely related to the elastic constants of the material [2]. With the application of pressure to rocks, an increase in p-wave

velocity occurs as a result of the closure of microcracks. Velocity can then be used to infer stress; however, the relationship is not linear. Velocity typically levels out at high stress and may even drop prior to failure as microcracks begin to coalesce.

2.2. *Inversion Methods*

Inverse methods are used to generate tomograms due to the fact that tomography problems are ill-posed; there are usually an infinite number of solutions for a tomography problem because the problem will have more unknowns than data or because there may be more data than unknowns but the data is inconsistent. However, when other information about the problem is considered, only a few of these solutions are likely [3]. Velocity tomography relies on the measurement of the travel time of seismic rays from a source to a receiver. The travel times are organized into a matrix **T** (1 x N), the distances traveled in each voxel into another matrix, **D** (N x M), and a slowness matrix, **P**, (1 x M) is unknown, so that **P** can be calculated by multiplying the inverse of **D** by **T** as shown in equation 1, below [4].

$$P = D^{-1}T \quad (1)$$

Since **D** is often a singular matrix the calculation cannot be accomplished directly leading to the development of various inversion methods. Three inversion programs were implemented to produce the tomograms presented in this paper: GeoTom, SIMULPS, and TomoDD.

GeoTom is a commercially available program that implements an iterative inversion process, SIRT, Simultaneous Iterative Reconstructive Technique [5]. An initial velocity model is provided by the user and then modified. First, a set of travel times is calculated through the model, and these travel times are then subtracted from the measured times to determine a residual time [4]. These residual times are used to correct the model and the process is repeated. The user specifies the number of iterations, and determines whether straight or curved raypaths are assumed. A smoothing constant, which weights the velocity at a node by the velocities at surrounding nodes can also be applied.

SIMULPS, written by Evans, Eberhart-Phillips, and Thurber, and updated by others, was also developed for use in earthquake tomography. This program relocates seismic events, generates a velocity model, and allows for variable gridding [6].

TomoDD, written by Zhang and Thurber was developed for use in earthquake tomography. TomoDD is a double-difference method that jointly relocates events and determines a velocity model [7]. Double-difference tomography relies on the idea that if the distance between two seismic events is small compared to the distance from the events to the receivers they will have similar travel times. Thus, the difference between calculated and measured travel times between two events at one receiver can be used to adjust the position of the events [8]. TomoDD allows for variable gridding, the interval between the x-, y-, and z- nodes in the inversion grid can be varied so that a finer grid may be applied in areas that are well sampled and a more course grid in areas that are not as well sampled. This is especially useful for passive sources because raypath density is rarely consistent.

Both SIMULPS and TomoDD use a damped-least-squares inversion. Damped-least-squares combines the squared data misfit with the norm of the model perturbations and minimizes them at each iteration [6]. A damping factor is input by the user for both TomoDD and SIMULPS. In SIMULPS the damping factor is determined by examining a plot of the data misfit against the model variance [6]. The ideal damping value is in the "elbow" of this trade-off curve. In TomoDD examination of a condition number output by the program is used to determine the damping value. The condition number, the ratio of the smallest to largest eigenvalue, should be between 40 and 80 with damping values between 1 and 100 [8].

2.3. *Prior Applications of Tomography in Mining*

There are numerous examples of utilization of tomography to infer the state of stress at a mine in the literature [9-12]. There are several examples specific to longwall mines utilizing velocity tomography [13] and attenuation tomography [14-16]. However, very few examples of long-term time-lapse passive seismic tomography can be found [17-18]. Most of the studies employ active sources such as blasts or hammer strikes and are conducted over the short term. Active sources make long term studies impractical. By utilizing mining induced microseismic events as passive sources, long-term, remote studies are feasible.

3. SITE DESCRIPTION AND EXPERIMENTAL PROCEDURE

Tomograms were generated from seismic data collected at a longwall coal mine located in the Western United States. The mine is deep and overlain by massive strata, making it susceptible to bumps. The data were collected over an 18-day period in 1997 and included 172,632 P-wave arrival times from 11,696 microseismic events. Average overburden at the mine is 350 meters, with coal seam height ranging from 2.6 to 3.0 meters. The seam is overlain by 2-7 meters of sandstone and underlain by 35 meters of sandstone. The mine has experienced bumps in the past mainly in the tailgate entry.

The panel under investigation is 250 meters wide with a previously mined panel to the tailgate side and an unmined panel to the headgate side. Over the course of the study the face retreated 431 meters, averaging about

24 meters per day. Sixteen geophones were assembled on the surface above the panel to monitor and locate microseismic events. Figure 1 displays the panel geometry and relative receiver locations. The face retreated through a series of backfilled entries about halfway through the study. These entries were mined for escapeway purposes and are evident in Figure 1.

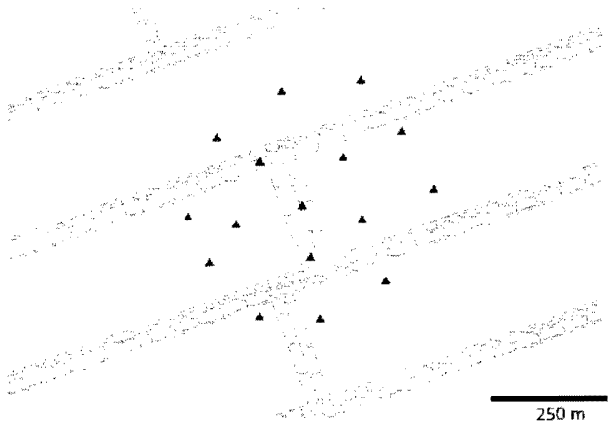

Figure 1. Outline of longwall panel and geophone locations. A series of back-filled entries is shown in the middle of the panel. Geophone locations shown as blue markers.

3.1. Data Reduction

The data set consists of event locations, station locations, seismic wave arrival times at stations, event magnitudes, and error values. Only events that reported arrival times by at least 10 of 16 stations were included in the set. A layered initial velocity model, determined from measurements at the site, was used. To convert arrival times to the travel times which are necessary for input to tomography, the ray that arrived to the station array first was propagated through the layered initial velocity model and assigned a travel time. This travel time was then added to the remaining arrival times for that event. Finally, any raypaths that had a velocity above 10,000 m/s were removed from the data sets. These velocities are likely the result of poor arrival time picks, and could produce high velocity artifacts in the tomograms. Pink phyllite has one of the highest p-wave velocities at 7,100 m/s [19], so a value of 10,000 m/s as the maximum reasonable velocity was chosen. Figure 2 shows a scatter plot of the travel times versus the distance between source and receiver. Examination of the plot shows that the background velocity is approximately 4500 meters/sec, the lowest observed velocities are approximately 3000 meters/sec and that the travel times above 10,000 meters/sec have been removed from the data set.

3.2. Inversion Parameters

Choosing the inversion parameters is one of the more complex aspects of seismic velocity tomography and is generally accomplished through trial and error, adjusting the input parameters and then evaluating output parameters. The parameters that are analyzed include the change in velocity values, which should be on the order of ten percent or less, and the overall "geologic reasonableness" of the results. Also, it is difficult to compare the parameters for different inversion methods. The most important input parameters in GeoTom are the smoothing constraints, the velocity range, and the number of curved and straight ray iterations. Travel time residuals are examined to determine if further changes should be made. A smoothing constant of 0.02 and 20 straight ray and 20 curved ray iterations was used. These values allowed the residuals to stabilize. Dines and Lytle indicate that while SIRT may take more time to converge to a solution than other iterative methods, the solution is stable [20]. For the data set an anisotropy factor of 1.1 was used. A value of 1.1 indicates that the waves travel 1.1 times faster parallel to the anisotropy vector than normal to the vector; this vector is near vertical. Values of 0.8 to 1.4 were tested and 1.1 minimized the travel time residuals. This data set included an anisotropy vector normal to the layers. Anisotropy refers to the variation of a characteristic of a material with the direction of measurement. An anisotropy value of 1.0 was determined to be sufficient for the other two data sets. In this case, p-wave velocity can vary as measured parallel or perpendicular to the bedding plane.

Important parameters in TomoDD include damping, weighting, and number of iterations. The damping factor damps the hypocentral adjustments if the adjustment vector becomes large or unstable. Damping factors between 120 and 150 were used resulting in condition numbers from 45 to 66. The weighting factors refer to smoothing in the x, y, and z directions and a

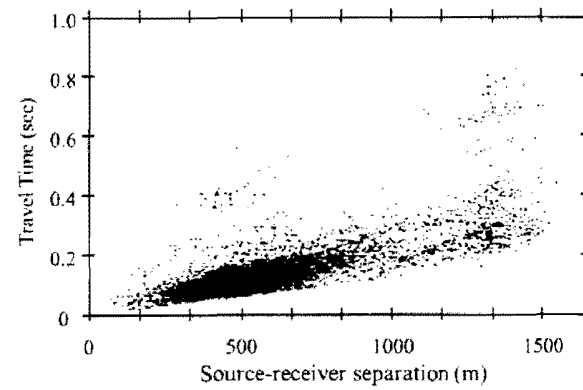

Figure 2. Scatter plot of distance between source and receiver vs. travel time.

factor of three was used. Thirty-two iterations were used. Both TomoDD and SIMULPS also relocate the microseismic events to better fit the model. In SIMULPS a damping parameter of 500 was used for the data set. This parameter was determined experimentally.

3.3. Display of Resulting Tomograms

Plan view velocity tomograms at seam level were generated. Pixels not traversed by rays are shown in purple. These zones vary significantly between inversion methods due to the variable gridding that is used in TomoDD and SIMULPS.

4. RESULTS AND DISCUSSION

Results were calculated for three days using each of the three inversion methods. The three days are listed in Table 1 along with the face advance, the previous day's face advance, and the number of events recorded on that day. This information is important because the rate of face advance can affect the stress redistribution; a high advance rate can result in higher stresses at the longwall face. The number of events used in SIMULPS and TomoDD can also affect the velocity range observed in the output. Although this can be compensated for by adjusting the damping parameters, it is preferable to be consistent. As can be seen in Table 1, the face advance rates and number of recorded events are comparable for the three days analyzed.

Table 1. Face advance rates and number of seismic events recorded for the three days included in the analysis.

Date	Face Advance (m)	Prior day's Face Advance (m)	Number of events recorded
July 26	25	15	739
August 1	29	18	819
August 6	30	15	847

Tomograms using the data for July 26, August 1, and August 6 were generated and are shown in Figure 3. Examination of the results from all three inversion methods reveals evidence of high velocity zones just ahead of the face and along the northern gateroad, corresponding with areas where front and tailside abutment stresses would be expected. Additionally, a low velocity zone can be seen just behind the face corresponding with the location of the gob. GeoTom, TomoDD, and SIMULPS all image high velocity zones in areas of side and forward abutment for the data. These features consistently redistribute with face advance and a low velocity zone in the gob area is also consistently present. Of the three days presented in Figure 3 tomograms are generated from over 8,000 raypaths.

The TomoDD tomograms seem to be more consistent from day to day for these data sets and agree most closely with the expected stress redistribution at the mine. Studies were conducted by personnel with the US Bureau of Mines at the mine to measure the forward abutment stress location [21]. Borehole pressure cells in the panel rib showed that the peak forward abutment stresses occurred within 5 m of the longwall face and stresses were not evident at a distance of 30 m from the face. This distribution is shown most clearly in the results obtained using the TomoDD, the double-difference passive seismic tomography method.

In comparing the three methods for the datasets it is evident that the methods that allow for variable gridding are more appropriate, especially for sparse data. However, even variable gridding does not allow very inconsistent data to be imaged well because a fine grid in one area will still result in some medium gridded areas that may not be sampled. Additionally, this research indicates that passive seismic velocity would not be appropriate for mines with relatively few mining induced microseismic events unless a dense receiver array is implemented. The data set shows that high velocity zones can be imaged in abutment stress areas and shown to redistribute using several different techniques. TomoDD proved to be the most suitable method for generating tomograms from mining-induced microseismic events because it resulted in the most consistent images and the calculated velocity distribution matched prior stress distribution measurements at the site.

5. SUMMARY AND CONCLUSIONS

Three seismic tomography methods were used to image the stress-induced velocity change at a longwall coal mine over a several week period. The goal of the study was to determine whether any of the methods produced results that were more repeatable and in agreement with previously measured stress redistribution. The three inversion methods included a simultaneous iterative reconstruction technique (GeoTom), a variably gridded local earthquake tomography method (SIMULPS), and a double-difference, variably gridded local earthquake tomography method (TomoDD). The data were collected at a deep longwall coal mine in the western United States. The results showed that all three methods imaged a high-velocity zone in the location of the forward and side abutments; however TomoDD had the most repeatable results and produced images that matched prior underground measurements most closely.

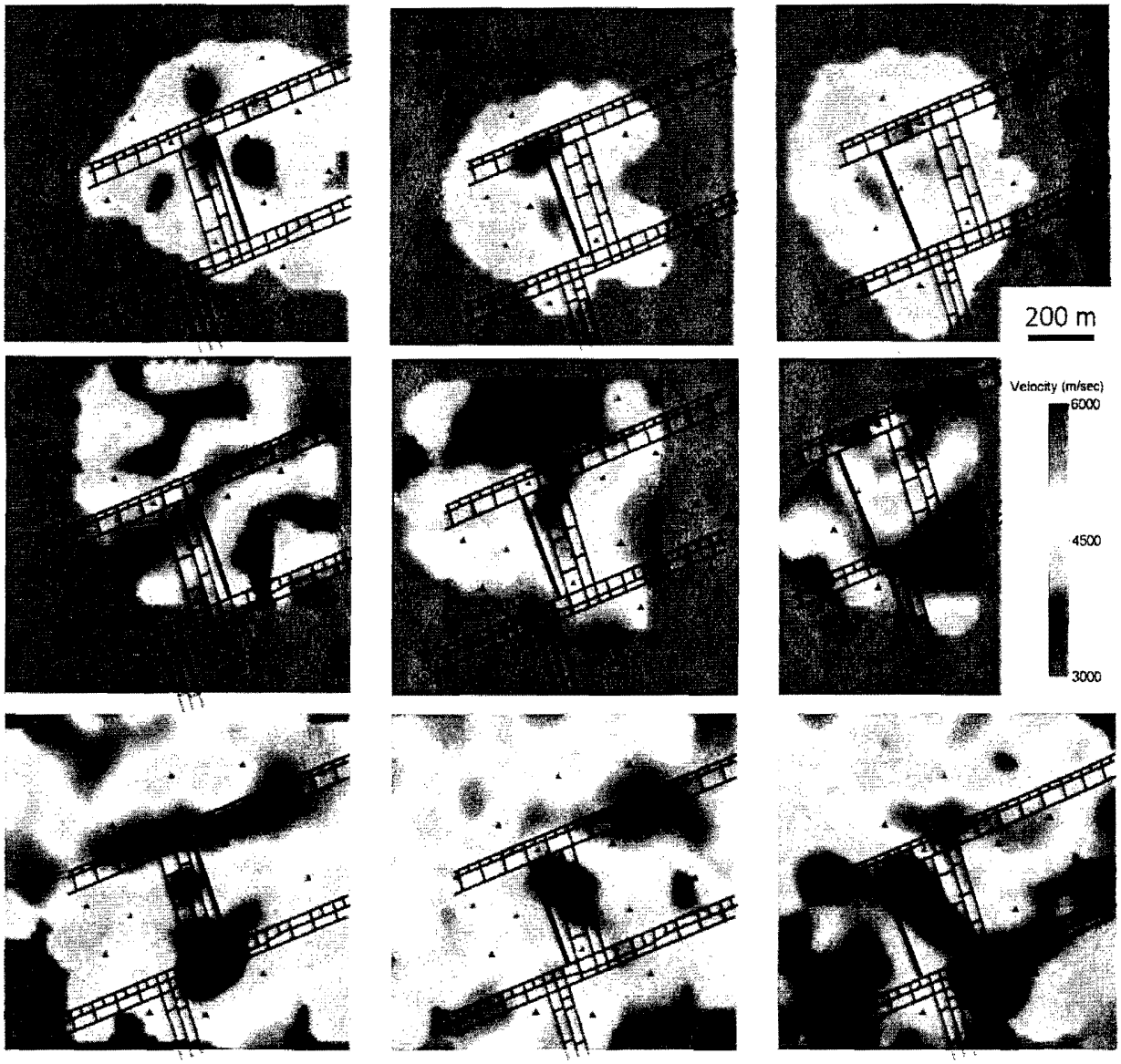

Figure 3. P-wave velocity tomography results for TomoDD (top row), SIMULPS (middle row), and Geotom (bottom row). Results for July 26 are in left column, for August 1 in central column, and for August 8 in right column. The location of the longwall mining face is shown for each day by the thick black line. The highly-stress forward abutment is clearly correlated to a high velocity region in the TomoDD results.

Based on these results, several conclusions can be drawn:

1) Passive seismic tomography can successfully produce time-lapse images of mining-induced stress redistribution at underground mines

2) The double-difference method (TomoDD) results in images that are more consistent and agree more closely with underground borehole pressure cell measurements than either the simultaneous iterative method or a non-double difference local earthquake tomography method (SIMULPS).

These conclusions support the continued use of double-difference passive seismic tomography for monitoring mining-induced stress redistribution in underground mines. This method provides pertinent information to the mine engineer regarding pillar design and abutment loading and also provides useful input to numerical modelers for calibration purposes. The ultimate goal of the work is to do all that is possible to ensure the safety of the underground miner.

ACKNOWLEDGEMENTS

The authors are grateful to the National Institute for Occupational Safety and Health for providing the raw data for this study and to Dr. Haijiang Zhang for sharing the passive seismic tomography code. This research was funded by a National Science Foundation CAREER grant (CMS-0134034).

REFERENCES

1. Cormack, A. 1969. Nobel Lecture: Early two-dimensional reconstruction and recent topics stemming from it. *Nobel Lectures, Physiology or Medicine* 1979-1980. Singapore, World Scientific Publishing Co.

2. Adams, L. and E. Williamson. 1923. On the compressibility of minerals and rocks at high pressures. *Journal of the Franklin Institute* 195: 475-531.

3. Hole, J. 1992. Nonlinear high-resolution three-dimensional seismic travel time tomography. *Journal of Geophysical Research* 97(B5): 6553-6562.

4. Jackson, M. and D. Tweeton. 1994. Report of Investigations 9497: MIGRATOM - Geophysical Tomography Using Wavefront Migration and Fuzzy Constraints. U.S. Dept. of the Interior, Bureau of Mines (Washington, D.C.).

5. Gilbert, P. 1972. Iterative methods for the three-dimensional reconstruction of an object from projections. *Journal of Theoretical Biology* 36: 105-117.

6. Evans, J., D. Eberhart-Phillips and C. Thurber. 1994. User's manual for SIMULPS12 for imaging vp and vp/vs: A derivative of the "Thurber" tomographic inversion SIMUL3 for local earthquakes and explosions. USGS.

7. Zhang, H. and C. Thurber 2003. Double-difference tomography: the method and its application to the Hayward Fault, California. *Bulletin of the Seismological Society of America* 93(5): 1875-1889.

8. Waldhauser, F. and W. Ellsworth. 2000. A double-difference earthquake location algorithm: method and application to the Northern Hayward Fault, California. *Bulletin of the Seismological Society of America* 90(6): 1353-1368.

9. Young, R. and S. Maxwell. 1992. Seismic characterization of a highly stressed rock mass using tomographic imaging and induced seismicity. *Journal of Geophysical Research* 97(B9): 12361-12373.

10. Maxwell, S. and R. Young. 1993. A comparison between controlled source and passive source seismic velocity images. *Bulletin of the Seismological Society of America* 83(6): 1813-1834.

11. Wright, C., E. Walls and D. d. J. Carneiro. 2000. The seismic velocity distribution in the vicinity of a mine tunnel at Thabazimbi, South Africa. *Journal of Applied Geophysics* 44: 369-382.

12. Scott, D., T. Williams, D. Tesarik, D. Denton, S. Knoll and J. Jordan. 2004. Geophysical methods to detect stress in underground mines: *Report of Investigations 9661*. NIOSH: 23.

13. Körmendi, A., T. Bodoky, L. Hermann, L. Dianiska and T. Kàlmàn. 1986. Seismic measurements for safety in Mines. *Geophysical Prospecting* 34: 1022-1037.

14. Hanna, K. and K. Haramy. 1998. Ground control and geologic assessment in mining through the use of geophysical tomographic imaging. *Geomechanics/Ground Control in Mining Underground Construction Conference*, Wollongong, NSW, Australia.

15. Westman, E., K. Heasley, P. Swanson and S. Peterson. 2001. A correlation between seismic tomography, seismic events, and support pressure. *38th U.S. Rock Mechanics Symposium, Washington, D.C.*, AA Balkema.

16. Hanson, D., T. Vandergrift, M. DeMarco and K. Hanna. 2002. Advanced techniques in site characterization and mining hazard detection for the underground coal industry. *International Journal of Coal Geology* 50: 275-301.

17. Glazer, S. and A. Lurka. 2007. Application of passive seismic tomography to cave mining operations based on experience at Palabora Mining Company, South Africa. *The Southern African Institute of Mining and Metallurgy 1st International Symposium on Block and Sub-Level Caving, Cape Town, South Africa.*

18. Luxbacher, K., E. Westman, P. Swanson and M. Karfakis. 2008. Three-dimensional time-lapse velocity tomography of an underground longwall panel. *International Journal of Rock Mechanics & Mining Sciences* 45(4): 478-485.

19. Carmichael, R. 1989. *Practical Handbook of Physical Properties of Rocks and Minerals*. Boca Raton, CRC Press.

20. Dines, K. and R. Lytle. 1979. Computerized geophysical tomography. *Proceedings of the IEEE* 67(7): 1065-1076.

21. Kneisley, R. O. and K. Haramy. 1992. Report of Investigations 9427: Large-scale strata response to longwall mining: a case study. U.S. Dept. of the Interior, Bureau of Mines (Washington, D.C.), 25 pp.

22. Swanson, P. 2008. Email: Simulps preliminary results. E. Westman. Blacksburg, VA.